

2x2-aperture 4-tap CMOS image sensor for multi-modal multi-band tissue imaging with suppressing the ambient light and motion artifact

Yuto Shimada¹, Kazuki Takada¹, Hoang Son Nam¹, Kakeru Miyazaki¹, Kohei Watanabe¹, Iori Shibata¹, Keita Yasutomi², Shoji Kawahito², Keiichiro Kagawa²

¹Graduate School of Integrated Science and Technology, Shizuoka Univ., Hamamatsu, 432-8011, Japan

²Research Institute of Electronics, Shizuoka Univ., Hamamatsu, 432-8011, Japan

E-mail: kagawa@idl.rie.shizuoka.ac.jp

I. INTRODUCTION

In this paper, a multi-aperture multi-tap CMOS image sensor for multi-modal quantitative wide-field tissue imaging is proposed. Simultaneous multi-modal image acquisition is effective for improving the accuracy of medical diagnosis. The proposed image sensor can perform multi-wavelength spatial frequency domain imaging (SFDI) with the structured light projection[1] and laser speckle contrast blood flow speed imaging (MELSCI)[2] for obtaining chromophore concentration, reduced scattering, and perfusion maps.

II. MULTI-APERTURE MULTI-TAP MULTI-MODAL CAMERA SYSTEM AND PRINCIPLE OF SFDI AND MELSCI

The concept of the tissue imaging camera is shown in Fig. 1. The image sensor area is divided into multiple regions, and each region is equipped with an optical filter and an imaging lens. Each region is separated by the image separator to avoid image overlapping. By using optical bandpass filters, multi-wavelength imaging and wavelength-division multiplexed imaging are possible. In Fig. 1, three different wavelengths are used for absorption and scattering imaging with SFDI, and the other wavelength is for blood

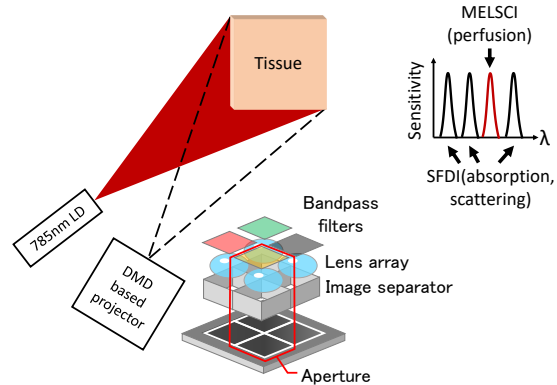


Fig. 1. Multi-modal tissue imaging system.

flow speed imaging with MELSCI.

SFDI is based on the fact that the modulation transfer function (MTF) of a scattering medium depends on the absorption coefficient μ_a and the reduced scattering coefficient μ'_s . The MTF for two or more spatial frequencies is measured at each pixel. Then, μ_a and μ'_s are estimated by referring to a look-up table made by the Monte Carlo simulation. To measure the MTF, three sinusoidal patterns with a one-dimensional wave vector whose spatial phases differ by $2\pi/3$ are projected to the tissue and their reflection images are taken. When the pixel values of the reflection images for the three spatial phases are denoted by $I_1(x, y)$, $I_2(x, y)$, and $I_3(x, y)$, the amplitude reflections

for AC and DC components, M_{AC} and M_{DC} , are calculated by Eqs. 1 and 2, respectively.

$$M_{AC} = (\sqrt{2}/3) [(I_1(x, y) - I_2(x, y))^2 + (I_2(x, y) - I_3(x, y))^2 + (I_3(x, y) - I_1(x, y))^2]. \quad (1)$$

$$M_{DC} = (1/3) [I_1(x, y) + I_2(x, y) + I_3(x, y)]. \quad (2)$$

MELSCI is a wide-field blood flow speed imaging method based on the bio-speckle by coherent illumination. When a laser beam is irradiated onto a scattering medium such as a tissue, the reflected light interferes on the imaging plane of the camera, producing a spatially random granular light intensity distribution called a speckle pattern. When red blood cells move by the blood flow, the speckle pattern changes over time. The speed of the change depends on the flow velocity. Since the speckle pattern is averaged over the exposure time of the image sensor, the faster the flow velocity becomes, the lower the spatial contrast does. The square speckle contrast $K^2(T)$ is defined by the following equation, where σ and $\langle I \rangle$ are the standard deviation and mean speckle intensity, respectively, for a region of interest.

$$K^2(T) = \frac{\sigma}{\langle I \rangle} \quad (3)$$

Fig. 2 shows a generally relationship between exposure duration and square speckle contrast value.

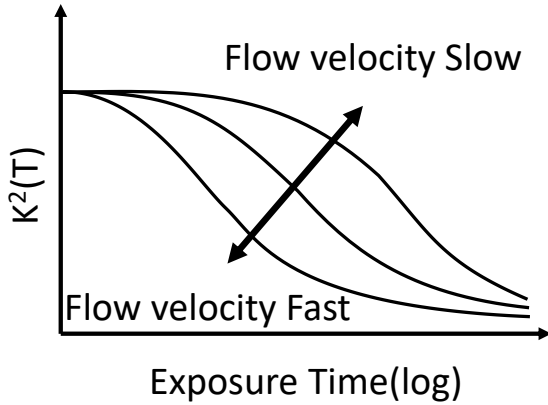


Fig. 2. K^2 value versus exposure time.

III. PROPOSED 2x2-APERTURE 4-TAP CMOS IMAGE SENSOR FOR MULTI-MODAL QUANTITATIVE WIDE-FIELD TISSUE IMAGING

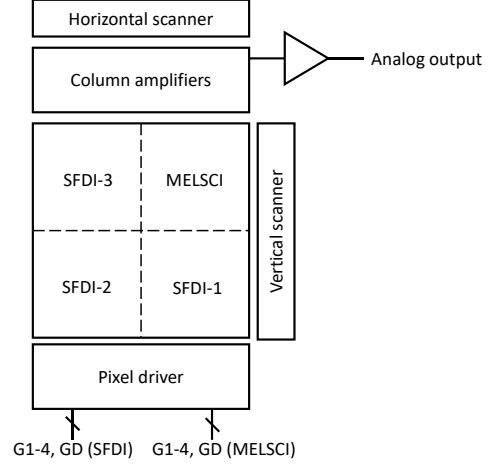


Fig. 3. Block diagram of the image sensor.

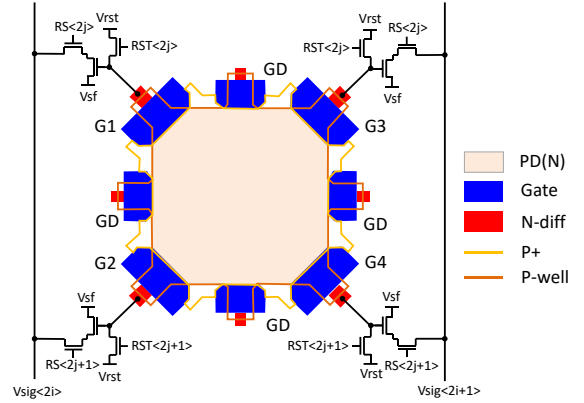


Fig. 4. Pixel structure.

The architecture of 2x2-aperture image sensor for tissue imaging is shown in Fig. 3. The proposed imaging device is composed of an array of sub-image sensors. This multi-aperture configuration enables multi-wavelength imaging to estimate chromophore concentrations and wavelength-division-multiplexed imaging of multi-band SFDI and MELSCI. Different exposure patterns can be applied to SFDI and MELSCI, respectively.

Fig. 4 shows the structure of the pixel with 4-taps and charge draining gates. Recently, multi-tap CMOS pixels for computational imaging have been studied [3-4]. The multi-tap pixels can simultaneously capture the multiple images

for different illuminations and exposure durations. Flexible exposure controllability of the multi-tap pixel is useful both for SFDI and MELSCI. We have demonstrated ambient light and motion artifact suppression in SFDI and efficient sampling with fewer exposures in MELSCI [5].

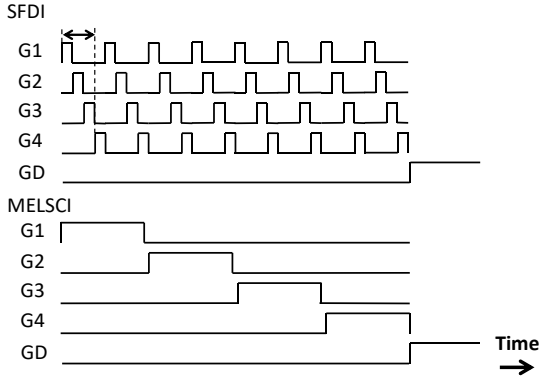


Fig. 5. Timing chart.

Fig. 5 shows an example timing chart of pixel operation. In SFDI, three patterns are projected sequentially, which are assigned to the taps-1 to -3, Tap-4 detects the ambient light. By shortening the unit exposure time and repeating the exposure, motion artifact of the measured optical property is suppressed while the captured image brightness is kept the same. The exposure of the MELSCI aperture should be independently controlled because the appropriate exposure time is optimized according to the flow speed range.

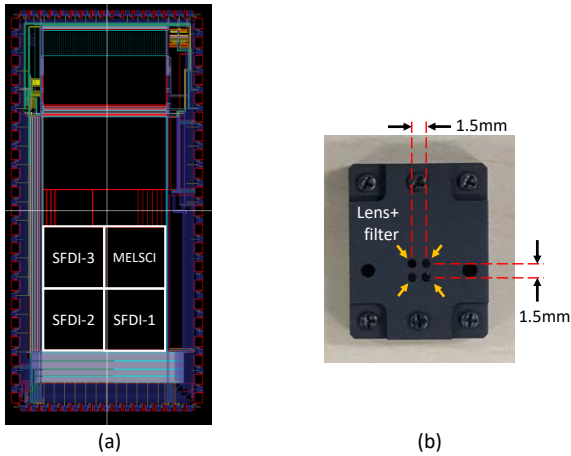


Fig. 6. (a) Image sensor layout and (b) attached optics.

Fig. 6(a) shows the layout of the prototype image sensor and the optics attached onto the image sensor. Table.1 summarizes the specifications and measured characteristics of the prototype.

Table 1. Specifications and characteristics

Technology	0.18 μ m CMOS process
Aperture count	2 \times 2
Pixel count per aperture	132 \times 132
Pixel size	11.2 μ m \square
Effective imaging area per aperture	1.48mm sq.
Fill factor	17.5%(w/o MLA)
Number of taps	4 taps + drain
Frame rate	2.8fps (limited by the output buffer problem)
Charge transfer speed	<10 μ s

IV. MEASUREMENT RESULTS

Fig. 7 shows the measured pixel response for the light pulse with a duration of 10 μ s and the wavelength of 445nm. The response is fast enough for the target application. A silicone phantom (6cm sq. and 2cm thickness) with different optical properties for the left and right sides was measured. The object moved at a speed of 0, 2, 4, 6, and 8mm/s. For SFDI, 450nm, 550nm, 660nm LEDs were used as light sources of the projector. For MELSCI, a 785nm LD was used for flood illumination. Fig. 8 shows an example of captured images. The unit exposure duration for SFDI and MELSCI was 10ms. Note that the spatial phases for the SFDI taps was different among the taps-1 to -3 images due to the switching of the projected patterns. The pattern was generated by a DMD. The spatial frequency of the projected sinusoidal patterns was 0.1mm⁻¹. Fig. 9 shows M_{DC} and M_{AC} maps under ambient light. The ambient light detected by tap-4 was subtracted from the other tap's images. It was shown that the retrieved optical property maps are not affected by the ambient light. Fig. 10 shows K^2 value maps. Note that K^2 value decreases as the exposure time or flow speed increases. Although those for 0mm/s should be the same for different synthesized exposure times, they are slightly different. This can be because of the read noise of the image sensor.

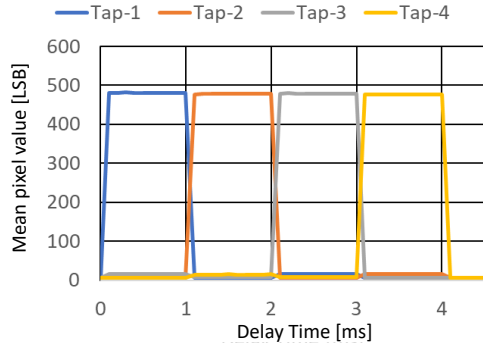


Fig. 7. Measured pixel response for the 10 μ s light pulse ($\lambda=445$ nm)

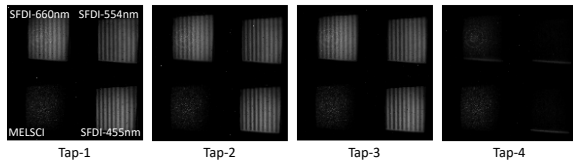


Fig. 8. Captured images for 0mm/s. (10 frames averaged)

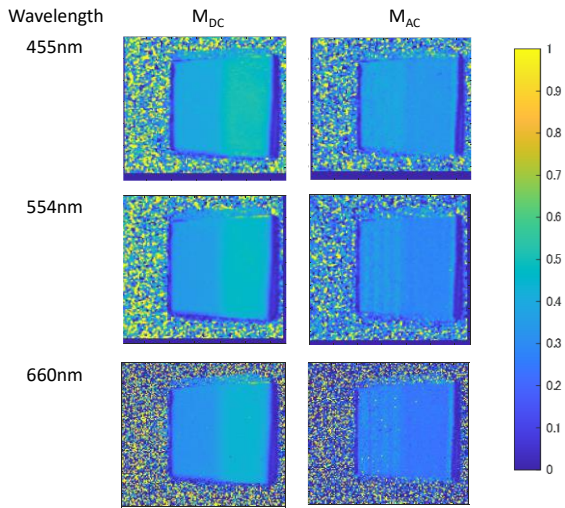


Fig. 9. Measured M_{DC} and M_{AC} maps from the images shown in Fig. 8.

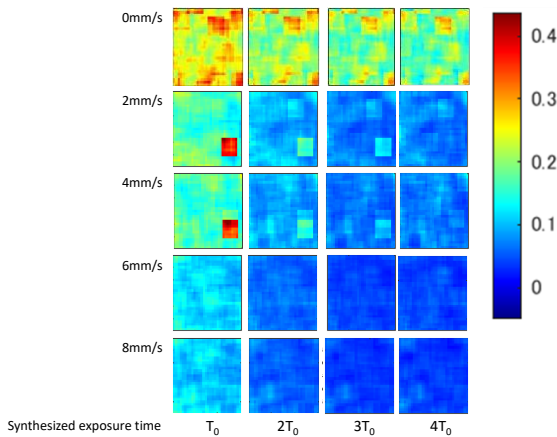


Fig. 10. Measured K^2 maps. $T_0=10$ ms.

V. CONCLUSIONS

In this paper, a 2x2-aperture 4-tap CMOS image sensor for multi-modal multi-band tissue imaging with suppressing the ambient light and motion artifact was proposed. We implemented different measurement methods: multi-band SFDI and MELSCI simultaneously. It was demonstrated that it was possible to simultaneously acquire wide-field maps of M_{DC} and M_{AC} and K^2 value of a silicone phantom.

ACKNOWLEDGMENTS

This work was supported in part by JSPS KAKENHI Grant Number 21H04557. This work was also supported by the VLSI Design and Education Center (VDEC), The University of Tokyo, in collaboration with Cadence Corporation, Synopsys Corporation, and Mentor Graphics Corporation. The image sensor was fabricated through the S-Project by Tohoku University.

REFERENCES

- [1] W. J. Tm *et al.*, "Robust flow measurement with multi-exposure speckle imaging," *Opt. Express*, Vol. 16, Issue 3, 1975 (2008).
- [2] D. J. Cuccia *et al.*, "Quantitation and mapping of tissue optical properties using modulated imaging," *J. Biomed. Opt.*, Vol. 14, 02412 (2009).
- [3] G. Wan *et al.*, "CMOS image sensors with multi-bucket pixels for computational photography," *IEEE J. Solid-State Circuits*, Vol. 47, No. 4, pp. 1031-1042 (2012).
- [4] T. Yoda *et al.* "The dynamic photometric stereo method using a multi-tap CMOS image sensor," *MDPI Sensors*, Vol. 18, 786 (2018).
- [5] K. Kagawa, "Functional imaging with multi-tap CMOS pixels," *ITE Transactions on Media Technology and Applications*, Vol. 9, Issue 2, pp. 114-121 (2021).